ACTIVE NOISE CONTROL OVER MULTIPLE REGIONS: PERFORMANCE ANALYSIS

Jihui Zhang, Huiyuan Sun, Prasanga N. Samarasinghe, Thushara D. Abhayapala
Acoustic & Audio Signal Processing Group, The Australian National University, Canberra ACT 2601, Australia

***Abstract*—Active noise control (ANC) over space is a well-researched topic where multi-microphone, multi-loudspeaker systems are designed to minimize the noise over a spatial region of interest. In this paper, we perform an initial study on the more complex problem of simultaneous noise control over multiple target regions using a single ANC system. In particular, we investigate the maximum active noise control performance over the multiple target regions, given a particular setup of secondary loudspeakers. The performance analysis is carried out using a wave-domain representation to best represent sound propagation over multiple regions in a given enclosure. Furthermore, given the global primary noise field and a fixed secondary source setup, a subspace method is exploited to evaluate the best system performance that could minimize the residual noise fields over multiple regions of interest. We provide experimental results to demonstrate the effectiveness of the proposed method.**

***Index Terms*—Active noise control, Multi-zone, Wave domain processing, Performance analysis**

I. Introduction

Spatial active noise control (ANC), creating large control area over 3D spatial regions, in applications such as noise cancellation in an aircraft or automobile [1]–[3], has been a growing research interest over recent years [4]. Spatial ANC utilizes a multichannel ANC system, which employs multiple secondary sources to cancel primary noise field over spatial regions [5]. The general multichannel ANC system has been implemented to cancel the noise at error sensors as well as their close surroundings [6]. Recently, wave domain signal processing has been applied to spatial ANC, which the noisefield over an entire region can be cancelled directly [7]–[11].

To analyse the spatial ANC performance, traditional methods evaluate the noise reduction on error microphone points [12] or on random points inside the region. These approaches can not directly indicate the performance over the entire spatial region. Chen et al. evaluated the spatial ANC performance using acoustic potential energy (APE) over spatial region, which provides a more robust and accurate evaluation [13]. Using the wave domain processing method, Zhang et al. investigated the maximum ANC performance over one single region for a given set of secondary sources in a particular environment [14].

Noise cancellation over multiple regions simultaneously using one ANC system has recently drawn attention due to a whole range of audio applications [15]. By cancelling the noise over multiple regions simultaneously, multiple listeners can be freely move between regions [16]. Recent work of multiple-zone soundfield control is formulated in modal domain based on spherical harmonic expansion, which provide theoretical insights of each region of interest [17]–[19]. Chen et al. investigated in-car noise cancellation performance by characterizing the noise pattern and averaging noise energy over multiple regions [20]. The fundamental limitation of noise reduction over multiple regions for a given single secondary loudspeaker array has not been developed yet.

In this paper, we analyse the spatial ANC performance over multiple regions of interest, for a given single secondary loudspeaker array in a particular environment. To best represent the sound field in each region of interest, we carry out the performance analysis using wave domain representation. We extract the subspace of the secondary path coefficients, and investigate the maximum noise reduction performance for each individual region by projecting the primary sound field into this subspace. We conduct experiment to demonstrate the potential application of the proposed subspace method.

II. Problem Formulation

In this section, we formulate the ANC problem in the wave domain to cancel the noise over multiple 3-D spatial regions.

Let the regions of interest be Z spherical regions with radius $[R_1, R_2, \cdots, R_Z]$, as shown in Fig. 1. Assume that the noise sources and L secondary sources are located outside the regions of interest. We measure the noise field by placing spherical microphone arrays on the boundary of the control regions. Any arbitrary observation point within the z^{th} control

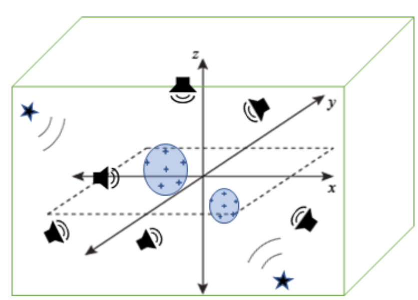

Fig. 1: ANC system in a 3-D room. Black stars represent primary sources, loudspeakers represent secondary sources, the blue spheres represent the regions of interest, and dark blue stars represent error microphones over the regions.

region is denoted as $\boldsymbol{x} \equiv \{r, \phi_{\boldsymbol{x}}, \psi_{\boldsymbol{x}}\}$. Here, r, ψ and ϕ are the

This research was funded by ARC Discovery Project Grant number DP180102375.

radius, elevation angle and the azimuthal angle with respect to the origin of the z^{th} region, respectively. In the ANC system, the residual signal at this point is given by

$$e^{(z)}(\boldsymbol{x},k) = \nu^{(z)}(\boldsymbol{x},k) + s^{(z)}(\boldsymbol{x},k), \tag{1}$$

where $k = 2\pi f/c$ is the wave number, f is the frequency, and c is the speed of sound propagation. $\nu^{(z)}(\boldsymbol{x},k)$ and $s^{(z)}(\boldsymbol{x},k)$ denote the primary noise field and the secondary sound field observed at point $\boldsymbol{x}$ of the z^{th} region, respectively.

The secondary sound field generated by a discrete loudspeaker array with L loudspeakers can be represented by

$$s(\boldsymbol{x},k) = \sum_{l=1}^{L} d_l(k) G(\boldsymbol{x}|\boldsymbol{y}_l,k), \tag{2}$$

where $d_l(k)$ is the driving signal for the l^{th} loudspeaker, $\boldsymbol{y}_l$ denotes the location of the l^{th} loudspeaker, and $G(\boldsymbol{x}|\boldsymbol{y}_l,k)$ denotes the acoustic transfer function (ATF) between the l^{th} loudspeaker and the observation point $\boldsymbol{x}$.

We then represent the primary noise field and secondary noise field in the wave domain.

The spherical harmonics based wave equation solution decomposes any incident wave field $\nu^{(z)}(\boldsymbol{x},k)$ observed at $\boldsymbol{x}$ into

$$\nu^{(z)}(\boldsymbol{x},k) = \sum_{n=0}^{\infty}\sum_{m=-n}^{n} \beta_{nm}^{(z)}(k) j_n(kr) Y_{nm}(\phi_{\boldsymbol{x}},\psi_{\boldsymbol{x}}), \tag{3}$$

where $j_n(\cdot)$ is the spherical Bessel function of order n and $Y_{nm}(\cdot)$ denotes the spherical harmonics. Therefore, the decomposition coefficients $\beta_{nm}^{(z)}(k)$ represent the primary noise field over the z^{th} region in the wave domain.

Within the z^{th} region of interest $r \le R_z$, a finite number of modes can be used to approximate the noise field [21]. Thus, the primary noise field in (3) can be truncated by

$$\nu^{(z)}(\boldsymbol{x},k) \approx \sum_{n=0}^{N_z}\sum_{m=-n}^{n} \beta_{nm}^{(z)}(k) j_n(kr) Y_{nm}(\phi_{\boldsymbol{x}},\psi_{\boldsymbol{x}}), \tag{4}$$

where the truncation order of $N_z = \lceil ekR_z/2 \rceil$ [21]–[23]. In the vector version, for all the regions of interest, $\boldsymbol{\beta}(k) = [\beta_{0,0}^{(1)}(k), \ldots, \beta_{N_1,N_1}^{(1)}(k), \ldots, \beta_{0,0}^{(Z)}(k), \ldots, \beta_{N_Z,N_Z}^{(Z)}(k)]^T$.

Using the spherical harmonic expansion, similar to the primary noise field, inside the z^{th} region of interest with the radius of R_z, the secondary sound field can be represented by

$$s^{(z)}(\boldsymbol{x},k) \approx \sum_{n=0}^{N_z}\sum_{m=-n}^{n} \gamma_{nm}^{(z)}(k) j_n(kr) Y_{nm}(\phi_{\boldsymbol{x}},\psi_{\boldsymbol{x}}). \tag{5}$$

The ATF in (2) can be parameterized in the wave domain as

$$G(\boldsymbol{x}|\boldsymbol{y}_l,k) \approx \sum_{n=0}^{N_z}\sum_{m=-n}^{n} \eta_{nm}^{(zl)}(k) j_n(kr) Y_{nm}(\phi_{\boldsymbol{x}},\psi_{\boldsymbol{x}}), \tag{6}$$

where $\eta_{nm}^{(zl)}(k)$ is the ATF in wave domain for each loudspeaker to each region of interest.

Substituting (6) and (5) into (2), the secondary sound coefficients $\gamma_{nm}(k)$ can also be represented by

$$\gamma_{nm}^{(z)}(k) = \sum_{l=1}^{L} d_l(k) \eta_{nm}^{(zl)}(k). \tag{7}$$

In matrix form, the relationship between the secondary source decomposition coefficients and the loudspeaker driving signals is given by

$$\boldsymbol{\gamma}(k) = \boldsymbol{\eta}(k)\boldsymbol{d}(k), \tag{8}$$

where

$$\boldsymbol{\eta}(k) = \begin{bmatrix} \boldsymbol{\eta}^{(1)}(k) & \boldsymbol{\eta}^{(2)}(k) & \cdots & \boldsymbol{\eta}^{(L)}(k) \end{bmatrix}, \tag{9}$$

with the dimension of $\sum_{z=1}^{Z}(N_z+1)^2 \times L$, and $\boldsymbol{d}(k) = [d_1(k), \ldots, d_L(k)]^T$. Here, for the l^{th} loudspeaker, $\boldsymbol{\eta}^{(l)}(k) = [\eta_{00}^{(1l)}(k), \cdots, \eta_{N_1N_1}^{(1l)}(k), \eta_{00}^{(2l)}(k), \cdots, \eta_{N_2N_2}^{(2l)}(k), \cdots, \eta_{00}^{(Zl)}(k), \cdots, \eta_{N_ZN_Z}^{(Zl)}(k)]^T$.

We investigate the maximum achievable ANC performance based on the primary noise field coefficients $\boldsymbol{\beta}(k)$ and the secondary-path information $\boldsymbol{\eta}(k)$ in the wave domain, and derive loudspeaker driving signals to achieve the maximum noise reduction performance over the multiple regions.

III. Maximum achievable ANC performance using subspace method

For a given ANC system setup in a given room environment, the secondary-path coefficient $\boldsymbol{\eta}(k)$ can be estimated. In this section, we extract the subspace spanned by the secondary-path coefficient, and only cancel the primary noise field which can be projected into this subspace.

A. Principal Component Analysis of the Secondary Path

In a given loudspeaker array setup, each column of matrix $\boldsymbol{\eta}(k)$ is not necessarily orthogonal. We perform the principal component analysis (PCA) of the correlation matrix $E\{\boldsymbol{\eta}^H(k)\boldsymbol{\eta}(k)\}$ to obtain an orthonormal eigen-basis for the space of the secondary path in the wave domain.

The correlation matrix $E\{\boldsymbol{\eta}^H(k)\boldsymbol{\eta}(k)\}$can be decomposed into a set of orthonormal eigenvectors and their corresponding eigenvalues, as follows:

$$E\{\boldsymbol{\eta}^H\boldsymbol{\eta}\} = \boldsymbol{U}\boldsymbol{\Lambda}\boldsymbol{V}, \tag{10}$$

where $\boldsymbol{U} = [\boldsymbol{u}_1, \ldots, \boldsymbol{u}_i, \ldots, \boldsymbol{u}_L]$ are the eigenvectors of the wave-domain ATF, $\boldsymbol{V} = \boldsymbol{U}^T$, and the i^{th} column corresponds to the eigenvalue λ_i. Here, the vectors $\boldsymbol{u}_1, \ldots, \boldsymbol{u}_i, \ldots, \boldsymbol{u}_L$ are written in order of descending eigenvalues $\boldsymbol{\Lambda}$ [24]. Depending on the acoustic environment and the loudspeaker placement, the first B components are used to represent the loudspeakers, which contain the most useful information. Then the corresponding eigenvectors are $\boldsymbol{U}^{\diamond} = [\boldsymbol{u}_1, \ldots, \boldsymbol{u}_B]$, where the dimension of $\boldsymbol{U}^{\diamond}$ is $L \times B$, and $B \le L$. Here onwards, the frequency dependent k is omitted for notational simplicity.

The subspace $\boldsymbol{O}$ spanned by the wave-domain secondary path coefficients $\boldsymbol{\eta}$ is defined as

$$\boldsymbol{O} = \boldsymbol{\eta}\boldsymbol{U}^{\diamond}. \tag{11}$$

By normalizing each column of matrix $\boldsymbol{O}$, the orthonormal vectors $\boldsymbol{o}_1, \ldots, \boldsymbol{o}_B$ are obtained. These vectors generate a subspace, which represents the loudspeaker array and the acoustic environment. The dimensions of basis $\boldsymbol{O}$ are $\sum_{z=1}^{Z} (N_z + 1)^2 \times B$.

For the l^{th} loudspeaker, in vector form, the average ATF coefficients over certain short frames can be represented as

$$\bar{\boldsymbol{\eta}}^{(l)} = \boldsymbol{O}\boldsymbol{\kappa}^{(l)}, \tag{12}$$

where $\boldsymbol{\kappa}^{(l)} = \{\kappa_1^{(l)}, \ldots, \kappa_b^{(l)}, \ldots, \kappa_B^{(l)}\}^T$ and $\kappa_b^{(l)}$ are the projection coefficients, $\kappa_b^{(l)} =< \boldsymbol{\eta}^{(l)}, \boldsymbol{o}_b >$. Here, $< \cdot, \cdot >$ is the inner product of two vectors.

Therefore, $\boldsymbol{\kappa} = \{\kappa^{(1)}, \ldots, \kappa^{(L)}\}$ is the secondary-path coefficients in the subspace $\boldsymbol{O}$, with the dimension of $B \times L$.

B. Projection of the Primary Noise Field into the Subspace

Below we project the wave-domain coefficients of the primary noise field $\boldsymbol{\beta}$ into the subspace $\boldsymbol{O}$.

The projection of a new primary noise field $\boldsymbol{\beta}$ into subspace $\boldsymbol{O}$ can be obtained by

$$\text{Proj}_{\boldsymbol{O}}\boldsymbol{\beta} = \sum_{b=1}^{B} < \boldsymbol{\beta}, \boldsymbol{o}_b > \boldsymbol{o}_b = \boldsymbol{O}\boldsymbol{y}, \tag{13}$$

where $\boldsymbol{y} = \{y_1, y_2, \ldots, y_B\}^T$ are the primary noise field coefficients in the subspace, and $y_b = < \boldsymbol{\beta}, \boldsymbol{o}_b >$.

Therefore, the primary noise field can be separated by two parts: the projected part and the remaining part,

$$\boldsymbol{\beta} = \text{Proj}_{\boldsymbol{O}}\boldsymbol{\beta} + R(\boldsymbol{\beta}), \tag{14}$$

where $R(\boldsymbol{\beta})$ is the orthogonal complement of the subspace $\boldsymbol{O}$. The projected part indicates the primary noise field which can be cancelled in this system setup, and the orthogonal complement indicates the primary noise field which can not be cancelled in this system. If $R(\boldsymbol{\beta}) = 0$, $\boldsymbol{\beta}$ lies in the subspace, then the primary noise field over the regions of interest can be completely cancelled by the loudspeaker array. In more general cases, $R(\boldsymbol{\beta}) \neq 0$. This indicates the limitation of noise cancellation over the regions of interest, under the particular loudspeaker placement and acoustic environment.

Next, we design the driving signal of loudspeaker $d_l(k)$ to cancel the primary noise field projected into the subspace.

C. Driving signal design in the subspace

In the subspace, matching the secondary sound field coefficients to the projected primary noise field coefficients, substituting (12) into (8), the optimal solution of the secondary sound field coefficients can be written by

$$\boldsymbol{\gamma} = -\text{Proj}_{\boldsymbol{O}}\boldsymbol{\beta} = \boldsymbol{O}\boldsymbol{\kappa}\boldsymbol{d}. \tag{15}$$

Substituting (13) into (15), the loudspeaker driving signals $\boldsymbol{d}$ can be calculated by

$$\boldsymbol{d} = -(\boldsymbol{\kappa})^{\dagger}\boldsymbol{y}, \tag{16}$$

where $(\boldsymbol{\kappa})^{\dagger}$ is the pseudoinverse of the secondary-path coefficients in the subspace, with the dimension of $L \times B$. The loudspeaker driving signals $\boldsymbol{d}$ are designed by the secondary-path information in the subspace $\boldsymbol{\kappa}$ and the primary noise field coefficients in the subspace $\boldsymbol{y}$, as shown in (16).

IV. Experiment

In this section, we conduct an experiment to evaluate the noise cancellation performance in a real room environment.

A. Experimental setup

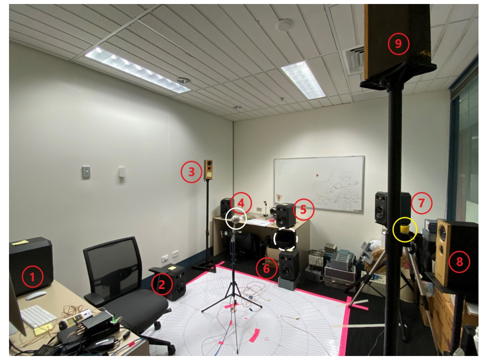

Fig. 2: Experimental setup in a reverberant room for an ANC system, with single noise source (yellow circle), 9 secondary loudspeakers (red circles) and an Eigenmike (white circle).

The experiment is carried out in an office room at the Australian National University with a size of $[3.54, 4.06, 2.70]$ m, as shown in Fig. 2. The origin of the room is the left-front-bottom corner. One loudspeaker is placed at two different locations (SP1: $[1.43, 3.78, 1.00]$ m and SP2: $[0.61, 1.10, 1.00]$ m) as the single noise source. White Gaussian noise has been used as primary noise signal to evaluate the ANC performance over [100, 500] Hz. 9 loudspeakers are used as secondary loudspeaker candidates with the random positions at [(3.11 3.37 1.22), (1.95 0.96 0.35), (3.08 3.24 0.30), (0.73 0.96 1.40), (3.22 1.18 1.78), (0.52 2.46 1.40), (3.22 0.60 1.10), (1.02 2.92 2.12), (2.14 0.60 1.10)] m. An Eigenmike [25] with $Q = 32$ microphones on a rigid sphere with $R = 0.042$ m is used as error microphone array, which the region of interest is inside the sphere. The Eigenmike is placed at $[2.64, 2.06, 1.15]$ m and $[1.72, 1.76, 0.93]$ m as the position of the two regions of interest.

We obtain the impulse response (IR) between each loudspeaker and the two regions of interest. We use the measured IRs to simulate the noise field in the regions of interest and to estimate secondary channels between the secondary loudspeakers and the error microphones. During the PCA process for the secondary path, components in $\boldsymbol{U}$ which correspond to λ_i occupying less than 5% of the largest eigenvalue $\boldsymbol{\lambda}_1$ are omitted in $\boldsymbol{U}^{\diamond}$.

To analyse the spatial ANC performance over multiple regions, we evaluate the APE within each spherical region [13]. The APE of residual signal over the z^{th} region can be represented by $E_p^{(z)}(k) = \frac{1}{4\rho c^2} \sum_{nm} w_n^{(z)} |\alpha_{nm}^{(z)}|^2$ [13], where $\alpha_{nm}^{(z)}$ denotes the error coefficient $\alpha_{nm}^{(z)} = \beta_{nm}^{(z)} + \gamma_{nm}^{(z)}$, and $w_n^{(z)}$

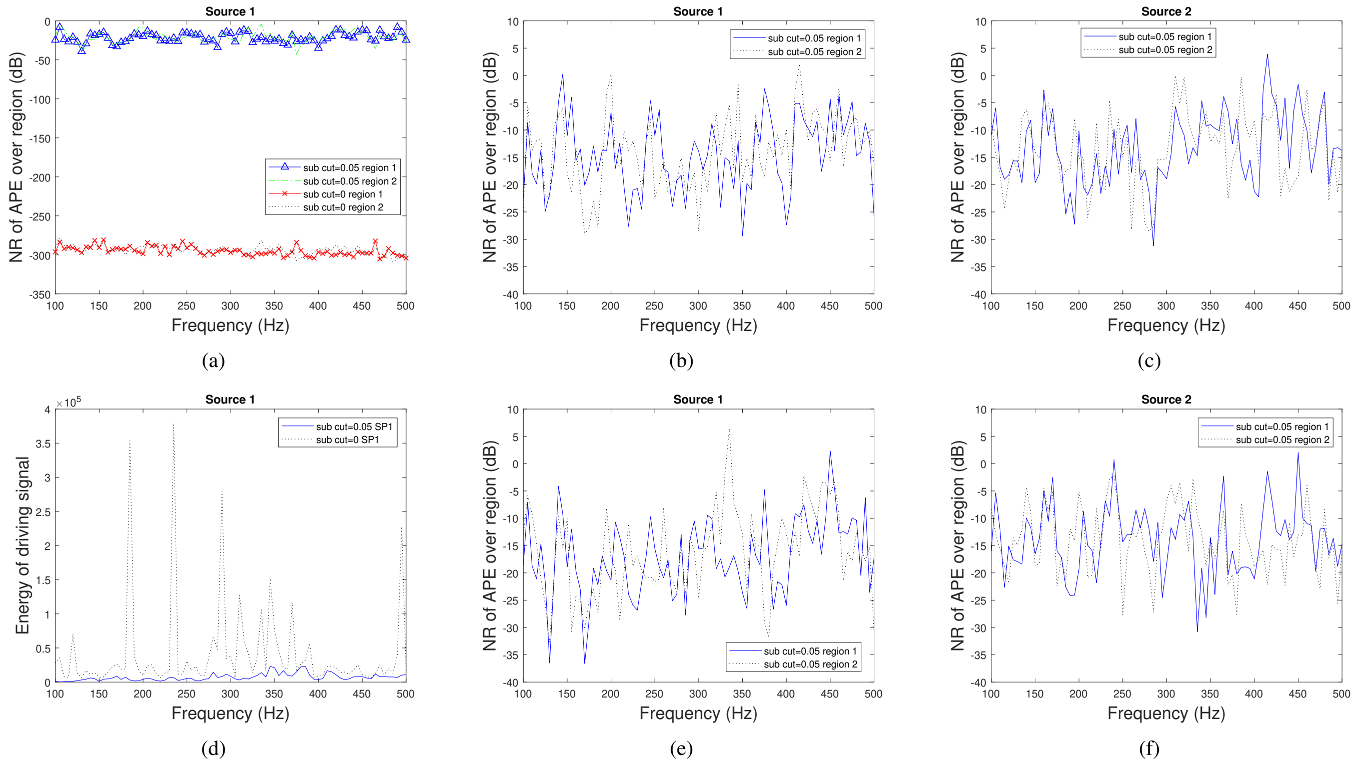

Fig. 3: When secondary loudspeakers [1:9] are active, (a) N_r for SP1, (d) E_d for SP1. When secondary loudspeakers [1:6] are active, (b) N_r for SP1, (c) N_r for SP2. When secondary loudspeakers [4:9] are active, (e) N_r for SP1, (f) N_r for SP2.

denotes the APE weights $w_n^{(z)} = \int_0^{R_z} j_n(kr)^2 r^2 dr$. Therefore we define the noise reduction over the z^{th} region as

$$N_{\text{r}}^{(\text{z})} \triangleq 10\log_{10}\frac{\sum_{nm} w_n^{(z)} |\alpha_{nm}^{(\text{z})}|^2}{\sum_{nm} w_n^{(z)} |\beta_{nm}^{(\text{z})}|^2}. \tag{17}$$

To evaluate the loudspeaker energy consumption, we use the total energy of all the loudspeakers $E_d = \boldsymbol{d}^T\boldsymbol{d}$.

B. *Experimental results*

In order to control all the modes in the two spatial regions, $2 \times (N+1)^2 = 8$ loudspeakers are required as secondary sources. In this section, we investigate loudspeaker number in two cases: $L = 9$, which meets the requirement; $L = 6$, which is less than the requirement.

1) Loudspeaker Number Meeting the Requirement: Fig. 3(a) and Fig. 3(d) demonstrate the noise reduction performance and the energy of all the loudspeakers when $L = 9$. Using the subspace analysing method, in both regions of interest, when we omit the less significant component in basis $\boldsymbol{u}$, N_r (blue and red) is less than the results when we keep all the component (green and black). While the high noise reduction when we reserve all the information is not physically achievable as the energy of driving signal at some frequency bins are very high, which will result in overloading of the secondary sources.

2) Loudspeaker Number Less Than the Requirement: Fig. 3(b), 3(c), 3(e), and 3(f) demonstrate the ANC performance over each region when $L = 6$. In Fig.3(b) and Fig 3(c), loudspeaker [1:6] are active; in Fig. 3(e) and Fig 3(f), loudspeaker [4:9] are active. When the loudspeaker number is less than the requirement, by evaluating the noise reduction over each individual region, we can determine better loudspeaker setup suitable for particular noise field.

V. Conclusion

This paper proposed an evaluation method for analysing the spatial active noise control performance over multiple regions. By projecting the primary sound field to a subspace generated by the wave domain coefficients of the secondary loudspeakers, we analysed maximum noise reduction over multiple regions for a given loudspeaker array setup with a feasible solution. For a given number of secondary loudspeakers, especially when the secondary sources have constraints on numbers and locations, using the proposed subspace method, we can analyse better locations to cancel a given primary sound field over multiple regions. The experimental results illustrate the potential applications for the proposed method. In this work, spherical microphone array has been distributed on the boundary of each region of interest. It is suggested that an investigation of spatial ANC performance over multiple regions by analysing sound acquisition capability of non-spherical microphone array is a topic of future work.

References

[1] J. Cheer and S. J. Elliott, “The design and performance of feedback controllers for the attenuation of road noise in vehicles,” *International Journal of Acoustics and Vibration*, vol. 19, no. 3, pp. 155–164, Jan. 2014.

[2] ——, “Multichannel control systems for the attenuation of interior road noise in vehicles,” *Mechanical Systems and Signal Processing*, vol. 60 61, pp. 753 – 769, 2015.

[3] P. N. Samarasinghe, W. Zhang, and T. D. Abhayapala, “Recent advances in active noise control inside automobile cabins: Toward quieter cars,” *IEEE Signal Processing Magazine*, vol. 33, no. 6, pp. 61–73, 2016.

[4] J. Zhang, T. D. Abhayapala, W. Zhang, P. N. Samarasinghe, and S. Jiang, “Active noise control over space: A wave domain approach,” *IEEE/ACM Transactions on Audio, Speech, and Language Processing*, vol. 26, no. 4, pp. 774–786, 2018.

[5] Y. Kajikawa, W.-S. Gan, and S. M. Kuo, “Recent advances on active noise control: open issues and innovative applications,” *APSIPA Transactions on Signal and Information Processing*, vol. 1, 2012.

[6] J. Tao, Q. Guo, and X. Qiu, “A near-field error sensing strategy for compact multi-channel active sound radiation control in free field,” *The Journal of the Acoustical Society of America*, vol. 146, no. 4, pp. 2179–2187, 2019.

[7] J. Zhang, W. Zhang, and T. D. Abhayapala, “Noise cancellation over spatial regions using adaptive wave domain processing,” in *2015 IEEE Workshop on Applications of Signal Processing to Audio and Acoustics (WASPAA)*, New Paltz, NY, USA, pp. 1–5.

[8] W. Zhang, C. Hofmann, M. Buerger, T. D. Abhayapala, and W. Kellermann, “Spatial noise-field control with online secondary path modeling: A wave-domain approach,” *IEEE/ACM Transactions on Audio, Speech, and Language Processing*, vol. 26, no. 12, pp. 2355–2370, 2018.

[9] Y. Maeno, Y. Mitsufuji, and T. D. Abhayapala, “Mode domain spatial active noise control using sparse signal representation,” in *2018 IEEE International Conference on Acoustics, Speech and Signal Processing (ICASSP)*, Calgary, Alberta, Canada, pp. 211–215.

[10] N. Murata, J. Zhang, Y. Maeno, and Y. Mitsufuji, “Global and local mode-domain adaptive algorithms for spatial active noise control using higher-order sources,” in *2019 IEEE International Conference on Acoustics, Speech and Signal Processing (ICASSP)*, Brighton, UK, pp. 526–530.

[11] H. Ito, S. Koyama, N. Ueno, and H. Saruwatari, “Feedforward spatial active noise control based on kernel interpolation of sound field,” in *2019 IEEE International Conference on Acoustics, Speech and Signal Processing (ICASSP)*, Brighton, UK, pp. 511–515.

[12] S. C. Douglas, “Fast implementations of the filtered-x lms and lms algorithms for multichannel active noise control,” *IEEE Transactions on Speech and Audio Processing*, vol. 7, no. 4, pp. 454–465, 1999.

[13] H. Chen, J. Zhang, P. N. Samarasinghe, and T. D. Abhayapala, “Evaluation of spatial active noise cancellation performance using spherical harmonic analysis,” in *2016 IEEE International Workshop on Acoustic Signal Enhancement (IWAENC)*, Xi’an, China, Sep. 2016, pp. 1–5.

[14] J. Zhang, T. D. Abhayapala, W. Zhang, and P. N. Samarasinghe, “Active noise control over space: A subspace method for performance analysis,” *Applied Sciences*, vol. 9, no. 6, p. 1250, 2019.

[15] T. Betlehem, W. Zhang, M. A. Poletti, and T. D. Abhayapala, “Personal sound zones: Delivering interface-free audio to multiple listeners,” *IEEE Signal Processing Magazine*, vol. 32, no. 2, pp. 81–91, 2015.

[16] W. Zhang, P. N. Samarasinghe, H. Chen, and T. D. Abhayapala, “Surround by sound: A review of spatial audio recording and reproduction,” *Applied Sciences*, vol. 7, no. 5, p. 532, 2017.

[17] Y. J. Wu and T. D. Abhayapala, “Spatial multizone soundfield reproduction: Theory and design,” *IEEE Transactions on audio, speech, and language processing*, vol. 19, no. 6, pp. 1711–1720, 2010.

[18] M. A. Poletti and F. M. Fazi, “An approach to generating two zones of silence with application to personal sound systems,” *The Journal of the Acoustical Society of America*, vol. 137, no. 2, pp. 598–605, 2015.

[19] W. Zhang, T. D. Abhayapala, T. Betlehem, and F. M. Fazi, “Analysis and control of multi-zone sound field reproduction using modal-domain approach,” *The Journal of the Acoustical Society of America*, vol. 140, no. 3, pp. 2134–2144, 2016.

[20] H. Chen, P. Samarasinghe, and T. D. Abhayapala, “In-car noise field analysis and multi-zone noise cancellation quality estimation,” in *2015 Asia-Pacific Signal and Information Processing Association Annual Summit and Conference (APSIPA)*, Hong Kong, China, pp. 773–778.

[21] R. Kennedy, P. Sadeghi, T. D. Abhayapala, and H. M. Jones, “Intrinsic limits of dimensionality and richness in random multipath fields,” *IEEE Transactions on Signal Processing*, vol. 55, no. 6, pp. 2542–2556, June 2007.

[22] T. D. Abhayapala, T. Pollock, and R. Kennedy, “Characterization of 3D spatial wireless channels,” in *2003 IEEE 58th Vehicular Technology Conference VTC 2003-Fall*, vol. 1, Orlando, FL, USA, Oct. 2003, pp. 123–127.

[23] R. A. Kennedy and T. D. Abhayapala, “Spatial concentration of wavefields : Towards spatial information content in arbitrary multipath scattering,” in *4th Australian Communications Theory Workshop (AusCTW)*, 2003, pp. 4–5.

[24] S. Wold, K. Esbensen, and P. Geladi, “Principal component analysis,” *Chemometrics and Intelligent Laboratory Systems*, vol. 2, no. 1, pp. 37–52, 1987.

[25] “em32 eigenmike microphone array release notes,” 2013. [Online]. Available: www.mhacoustics.com/sites/default/files/ReleaseNotes.pdf